Computers and Concrete, *Vol. 26, No. 3* (*2020*) *213-226*
DOI: https://doi.org/10.12989/cac.2020.26.3.213

Deflections, stresses and free vibration studies of FG-CNT reinforced sandwich plates resting on Pasternak elastic foundation

Noureddine Bendenia[1], Mohamed Zidour[2], Abdelmoumen Anis Bousahla*[3], Fouad Bourada[1,4], Abdeldjebbar Tounsi[1], Kouider Halim Benrahou[1], E.A. Adda Bedia[5], S.R. Mahmoud[6] and Abdelouahed Tounsi[1,5]

[1]*Material and Hydrology Laboratory, Faculty of Technology, Civil Engineering Department, University of Sidi Bel Abbes, Algeria*
[2]*Laboratory of Geomatics and Sustainable Development, University of Tiaret, Algeria*
[3]*Laboratoire de Modélisation et Simulation Multi-échelle, Université de Sidi Bel Abbés, Algeria*
[4]*Département des Sciences et de la Technologie, Centre Universitaire de Tissemsilt, BP 38004 Ben Hamouda, Algérie*
[5]*Department of Civil and Environmental Engineering, King Fahd University of Petroleum & Minerals, 31261 Dhahran, Eastern Province, Saudi Arabia*
[6]*GRC Department, Jeddah Community College, King Abdulaziz University, Jeddah, Saudi Arabia*

(*Received May 3, 2020, Revised August 4, 2020, Accepted August 5, 2020*)

Abstract. The present study covenants with the static and free vibration behavior of nanocomposite sandwich plates reinforced by carbon nanotubes resting on Pasternak elastic foundation. Uniformly distributed (UD-CNT) and functionally graded (FG-CNT) distributions of aligned carbon nanotube are considered for two types of sandwich plates such as, the face sheet reinforced and homogeneous core and the homogeneous face sheet and reinforced core. Based on the first shear deformation theory (FSDT), the Hamilton's principle is employed to derive the mathematical models. The obtained solutions are numerically validated by comparison with some available cases in the literature. The elastic foundation model is assumed as one parameter Winkler - Pasternak foundation. A parametric study is conducted to study the effects of aspect ratios, foundation parameters, carbon nanotube volume fraction, types of reinforcement, core-to-face sheet thickness ratio and types of loads acting on the bending and free vibration analyses. It is explicitly shown that the (FG-CNT) face sheet reinforced sandwich plate has a high resistance against deflections compared to other types of reinforcement. It is also revealed that the reduction in the dimensionless natural frequency is most pronounced in core reinforced sandwich plate.

Keywords: nanotubes; deflections; Pasternak; functionally graded; sandwich

1. Introduction

Composite materials are playing an increasingly important role in the production of structures with high mechanical performance (aerospace, aeronautics, automotive) and have greatly contributed to the development of our technologies. Polymeric and laminated composite materials stand out for their lightness and ease of use. Their mechanical, physical and chemical resistances offer a wide range of possibilities in terms of use, design, geometry and integration of functions and have been replacing the conventional materials. The use of nanofillers, in particular graphene, carbon nanotubes, fullerenes, carbon nanofibers, graphite; makes it possible to manufacture new high-performance composite materials called nanocomposites, because of their excellent mechanical, thermal, electrical and optical properties. This allows for many applications in the industrial sectors. There are many scientific papers in the literature which investigate the mechanical behavior of the composites and nanocomposites structures in various scales (Avcar *et al*. 2016, Avcar and Mohammed 2018, Behera and Kumari 2018, Narwariya *et al*. 2018, Monge *et al*. 2019, Bakhshi and Taheri-Behrooz 2019, Ghannadpour and Mehrparvar 2020, Shokrieh and Kondori 2020, Abed and Majeed 2020, Katariya *et al*. 2020). Ajayan *et al*. (1994) investigated the nanocomposites (CNTRCs) made from polymer reinforced by aligned CNT arrays. Fidelus *et al*. (2005) presented the Thermomechanical properties of nanocomposites made from epoxy and oriented carbon nanotubes. A numerical simulation was performed using dynamic finite element to analyses the response of laminated composite plates under low-velocity impact loading by Aslan *et al*. (2003). To investigate the wave propagation in laminated and sandwich composite strips a layerwise semi-analytical method is proposed by Barouni and Saravanos (2016). Mirzaei and Kiani (2016) developed the thermal buckling analysis of FG-CNT reinforced composite plates. Verma (2013) employed three-dimensional filed equations to study the dispersion of wave probagation in an arbitrary direction in laminated composite plates. With a circular cross section reinforced by a single-walled carbon nanotube Vodenitcharova and Zhang (2006) sought a model for pure bending of a straight nanocomposite beam. Al-Osta *et al*. (2019) investigated the shear behaviour of RC beams retrofitted using UHPFRC panels epoxied to the sides. Panjehpour *et al*. (2018) developed the structural Insulated Panels. The effect of rotation and gravity on generalized

*Corresponding author, Ph.D.
E-mail: bousahla.anis@gmail.com

Copyright © 2020 Techno-Press, Ltd.

ISSN: 1598-8198 (Print), 1598-818X (Online)

thermo-viscoelastic medium with voids was performed by Othman *et al*. (2018). Functionally graded materials (FGMs) are new type of composite developed recently; he has high potential to use as a structural material. Ahmed *et al*. (2019) presented the post-buckling behavior of continuously graded FG nanobeams with geometrical imperfections. Mirjavadi *et al*. (2019) developed the dynamic response of metal foam FG porous cylindrical micro-shells.

Functionally graded carbon nanotube (FG-CNT) distributions along the transverse direction of structure have shown increasing attention in the past years. Zhang *et al*. (2015) used an element-free approach to investigate the buckling of FG-CNT reinforced composite thick skew plates. The kp-Ritz method is employed by Lei *et al*. (2015) to examine the free vibration of FG-CNT reinforced composite plates. The shear buckling of reinforced composite plates using Chebyshev-Ritz method is studied by Kiani (2016). The thermal and mechanical stability of (FG CNT)-reinforced composite surrounded by the elastic foundations truncated conical shells was studied by Duc *et al*. (2017). Mohammadzadeh-Keleshteri *et al*. (2017) extended the idea of FGMs to FG-CNTRCs to study the nonlinear free vibration of reinforced composite annular sector plates integrated with piezoelectric layers. Mehar and Panda (2017a) presented under various loadings and shear deformable an analysis of thermoelastic of FG-CNT reinforced composite plate. A numerical study of supersonic FG-CNT reinforced composite flat panels in thermal environments was performed by Asadi *et al*. (2017). Madani *et al*. (2016) employed a differential cubature method for examined under uniform and non-uniform temperature distributions, the vibration of embedded FG-CNT-reinforced piezoelectric cylindrical shells. Using integrated piezoelectric layers on elastic foundation, Keleshteri *et al*. (2017) investigated the large amplitude vibration of FG-CNT reinforced composite annular plates. Sahmani and Fattahi (2017) employed an exponential shear deformable and nonlocal size dependency for nonlinear instability of axially loaded FG-CNT reinforced nanoshells under heat conduction. Under elevated non-uniform temperature fields, Static behavior of FG-CNT polymer nano composite plate was studied by Jeyaraj and Rajkumar (2013). To a peculiarity analysis, Mehar and Panda (2018a) presented a thermoelastic flexural of FG-CNT doubly curved shell panel. In addition, few experimental, numerical and simulation articles on the CNT, Graded CNT, Graded structure and Sandwich are developed recently (Panda and Singh 2010, Panda and Katariya 2015, Kar *et al*. 2015, Sahoo *et al*. 2016, 2017, Lal *et al*. 2017, Mehar *et al*. 2017, 2018, Kiani *et al*. 2018, Mehar and Panda 2017b, 2018b, Katariya *et al*. 2018, Kiani 2017a, b, c, 2018, Rezaiee-Pajand *et al*. 2018, Dihaj *et al*. 2018, Hamidi *et al*. 2018, Katariya and Panda 2019a, b, Kunche *et al*. 2019, Hirwani and Panda 2019, Safa *et al*. 2019, Sahouane *et al*. 2019, Hadji *et al*. 2019, Sayyad and Ghumare 2019, Sahu *et al*. 2020, Dewangan *et al*. 2020, Merzoug *et al*. 2020, Rachedi *et al*. 2020, Mehar and Panda 2020, Anil *et al*. 2020, Pandey *et al*. 2019, 2020, Abdulrazzaq *et al*. 2020a, b, Al-Maliki *et al*. 2020, Rahmani *et al*. 2020, Al-Maliki *et al*. 2020, Patnaik *et al*. 2020, Mehar *et al*. 2020ab).

The large number of researchers who studied FG-CNT based on Nanotubes as reinforcement. The superlative properties of this material make it an excellent reinforcement for polymer matrix. Cooper *et al*. (2002) and Barber *et al*. (2003), which demonstrated that carbon nanotubes are effective in reinforcing a polymer due to remarkably high separation stress according to a series of pull-out tests of individual carbon nanotubes embedded within polymer matrix. The constitutive models and mechanical properties of carbon nanotube have been studied analytically, experimentally, and numerically. Xie *et al*. (2000) examined the mechanical and physical properties of carbon nanotube. A fundamental transmitting properties of carbon nanotube antennas is studied by Hanson (2005). Hone *et al*. (2000) carried out the electrical and thermal transport properties of magnetically aligned single wall carbon nanotube films. The double-walled carbon nanotube with surrounding elastic medium under axial pressure was performed by Ranjbartoreh *et al*. (2007). The buckling analysis of embedded concrete columns armed with carbon nanotubes was presented by Arani and Kolahchi (2016).

Sandwiches are interest for applications that require both rigidity and lightness. Their low self-weight is considered a remarkable advantage compared with traditional structures. They consist of two skins spaced from each other by thick core. The nanocomposite sandwiches composed of two phases which are polymer matrix and dispersed phase of carbon nanotubes (CNT). The sandwich structures received increasing attention due to their superior characteristics. The mechanical Properties of L-joint with composite sandwich structure is studied by Li *et al*. (2019).

Shokravi (2017) employed a Reddy plate theory to investigated the buckling of (FG-CNT)-reinforced sandwich plates resting on orthotropic elastic medium. In recent years, many paper investigated the mechanical behavior of sandwich or other structures such as: Static analysis (Dash *et al*. 2019, Mahapatra *et al*. 2017), bending and buckling analysis (Hamed *et al*. 2020, Eltaher and Mohamed 2020, Katariya *et al*. 2017) and vibrational behaviors (Selmi 2019, Barati 2019, Nejadi and Mohammadimehr 2020, Gafour *et al*. 2020).

There was no previous work done on the static and free vibration behavior of nanocomposite sandwich plates reinforced by carbon nanotubes resting on Pasternak elastic foundation. This present researches are investigated for the first time within the first shear deformation theory the static and free vibration problems of CNTRC plates reinforced by CNTs resting on Pasternak elastic foundation. The impacts of different parameters on the deflections, stresses and natural frequencies of such sandwich plates with facesheet reinforced and homogeneous core and the sandwich with homogeneous facesheet and reinforced core are introduced and examined according to several important aspects for example, plate thickness, aspect ratios, volume fraction of CNTs and sandwich plate types, etc. The numerical results are compared with those that are given in the literature.

2. Carbon nanotube reinforced composite sandwich plates

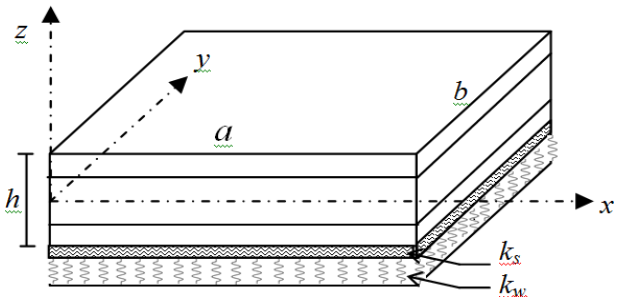

Fig. 1 Geometries of sandwich plate resting on Pasternak elastic foundatio

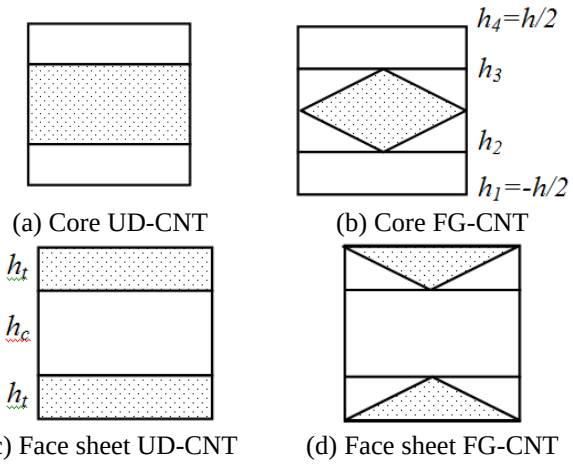

(a) Core UD-CNT (b) Core FG-CNT

(c) Face sheet UD-CNT (d) Face sheet FG-CNT

Fig. 2 Geometries of layers reinforced sandwich plate

As shown in Figs. 1 and 2, in this paper, the sandwich plate is made of two CNTRC face sheets with thickness of h_f and a stiff core layer of thickness h_c. Consider the case of a uniform thickness the sandwich plate composed three elastic layers denoted from bottom to top of the plate by h_1=-h/2, h_2, h_3, h_4=h/2.

The face sheet or core layers plates are assumed to be reinforced by two different types of aligned carbon nanotube distribution. UD-CNT represents the uniform distribution and FG-CNT the functionally graded distributions of carbon nanotubes in the thickness direction of the layers.

In the present study, the CNTRC material properties of the two-phase nanocomposites, mixture of CNTs and an isotropic polymer was employed by introducing the CNT efficiency parameters (η_1, η_2, η_3) in the rule of mixture. Considering that, the rule of mixture can be estimated according to the rule of mixture Esawi scheme (2007). According to the rule of mixture, the mechanical properties of the nanocomposite can be obtained by the following relations (Shen 2009).

$$E_{11} = \eta_1 V_{cnt} E_{11}^{cnt} + V_p E^p \tag{1a}$$

$$\frac{\eta_2}{E_{22}} = \frac{V_{cnt}}{E_{22}^{cnt}} + \frac{V_p}{E^p} \tag{1b}$$

$$\frac{\eta_3}{G_{12}} = \frac{V_{cnt}}{G_{12}^{cnt}} + \frac{V_p}{G^p} \tag{1c}$$

Table 1 The CNT efficiency parameters (η)

Case	η_1	η_2=η_3
V_{cnt}^*=0.11	0.149	0.934
V_{cnt}^*=0.14	0.150	0.941
V_{cnt}^*=0.17	0.149	1.381

Where $E_{11}^{cnt}, E_{22}^{cnt}$ and G_{12}^{cnt} indicate the Young's moduli and shear modulus of SWCNTs, respectively, and E^P and G^P represent the properties of the isotropic matrix. η_i (i=1,2,3) are the CNT efficiency parameters to consider the small scale effect. The V_{cnt} and V_p are the volume fractions of the carbon nanotubes and matrix, respectively, and it is noticeable that V_{cnt}+V_p=1. For other properties in terms of Poisson's ratio (ν) and mass density (ρ), these can be written as

$$\nu_{12} = V_{cnt}\nu_{12}^{cnt} + V_p\nu^p \quad , \quad \rho = V_{cnt}\rho^{cnt} + V_p\rho^p \tag{2}$$

In this research, it is supposed that for the FG-CNT the V_{cnt} volume fraction of aligned CNT was changed linearly by a function depicted in Fig. 2:

For UD-CNT reinforced sandwich plate

$$\left.\begin{aligned} V_{cnt} &= 0 \\ V_{cnt} &= V_{cnt}^* \end{aligned}\right\} \begin{aligned} &\text{for top and bottom face sheet} \\ &\text{for core} \end{aligned} \tag{3a}$$

$$\left.\begin{aligned} V_{cnt} &= V_{cnt}^* \\ V_{cnt} &= 0 \end{aligned}\right\} \begin{aligned} &\text{for top and bottom face sheet} \\ &\text{for core} \end{aligned} \tag{3b}$$

and also for FG-CNT reinforced sandwich plate

$$\left.\begin{aligned} V_{cnt} &= 0 \\ V_{cnt} &= 2\left(\frac{|z|}{h_2}+1\right)V_{cnt}^* \end{aligned}\right\} \begin{aligned} &\text{for top and bottom face sheet} \\ &\text{for core} \end{aligned} \tag{4a}$$

$$\left.\begin{aligned} V_{cnt} &= 2\left(\frac{h_2-|z|}{h_2-h_1}\right)V_{cnt}^* \\ V_{cnt} &= 0 \\ V_{cnt} &= 2\left(\frac{|z|-h_3}{h_4-h_3}\right)V_{cnt}^* \end{aligned}\right\} \begin{aligned} &\text{for bottom face sheet} \\ &\text{for core} \\ &\text{for top face sheet} \end{aligned} \tag{4b}$$

where V_{cnt}^* is the given volume fraction of CNTs, which can be obtained from the following equation

$$V_{cnt}^* = \frac{W_{cnt}}{\left(\frac{\rho^{cnt}}{\rho^m}\right) + \left(1-\frac{\rho^{cnt}}{\rho^m}\right)W_{cnt}} \tag{5}$$

Where W_{cnt} is the mass fraction of the carbon nanotube in the nano-composite plate, In this paper, Table 1 shows the efficiency parameters (η) associated with the given volume fraction $\left(V_{cnt}^*\right)$ (Zhu *et al*. 2012).

3. Theoretical formulations:

3.1 Displacement filed and strains of CNTRC plates

The present part is allocated to introduce a first order shear deformation plate theory (FSDT) in order to produce the equations of motion of the sandwich plate within a plate domain, according to displacements and rotations of the mid-plane of the plate. The displacement field based on the theory of a material point located at (x, y, z) in CNTRC sandwich plates is given below (Reddy 2004)

$$\begin{cases} u(x,y,z,t) = u_0(x,y,t) + z\varphi_x \\ v(x,y,z,t) = v_0(x,y,t) + z\varphi_y \\ w(x,y,t) = w_0(x,y,t) \end{cases} \tag{6}$$

Where u_0, v_0 and w_0 represent the respective translation along the x, y and z directions in the mid plane of the plate, t is time. Additionally, ϕ_x, ϕ_y denote the total bending rotation of the transverse normal about the y- and x-axis, respectively. If the last term in Eq. (6) is neglected, the displacements are reduced to the classical plate theory (CPT).

The linear in-plane and transverse shear strains can be expressed by following equations

$$\begin{Bmatrix} \varepsilon_{xx} \\ \varepsilon_{yy} \\ \gamma_{xy} \end{Bmatrix} = \begin{Bmatrix} \dfrac{\partial u_0}{\partial x} \\ \dfrac{\partial v_0}{\partial y} \\ \dfrac{\partial u_0}{\partial y} + \dfrac{\partial v_0}{\partial x} \end{Bmatrix} + z \begin{Bmatrix} \dfrac{\partial \varphi_x}{\partial x} \\ \dfrac{\partial \varphi_y}{\partial y} \\ \left(\dfrac{\partial \varphi_x}{\partial y} + \dfrac{\partial \varphi_y}{\partial x} \right) \end{Bmatrix} \tag{7}$$

$$\begin{Bmatrix} \gamma_{xz} \\ \gamma_{yz} \end{Bmatrix} = \begin{Bmatrix} \varphi_x + \dfrac{\partial w_0}{\partial x} \\ \varphi_y + \dfrac{\partial w_0}{\partial y} \end{Bmatrix}$$

3.2 The elastic stress-strain relations

The expression of elastic stress-strain relations of orthotropic composite materials is written in the form

$$\begin{Bmatrix} \sigma_{xx} \\ \sigma_{yy} \\ \sigma_{yz} \\ \sigma_{xz} \\ \sigma_{xy} \end{Bmatrix} = \begin{bmatrix} Q_{11} & Q_{12} & 0 & 0 & 0 \\ Q_{12} & Q_{22} & 0 & 0 & 0 \\ 0 & 0 & Q_{44} & 0 & 0 \\ 0 & 0 & 0 & Q_{55} & 0 \\ 0 & 0 & 0 & 0 & Q_{66} \end{bmatrix} \begin{Bmatrix} \varepsilon_{xx} \\ \varepsilon_{yy} \\ \varepsilon_{yz} \\ \gamma_{xz} \\ \gamma_{xy} \end{Bmatrix} \tag{8}$$

Where Q_{ij} are the transformed elastic constants

$$Q_{11} = \frac{E_{11}}{1-\upsilon_{12}\upsilon_{21}}, Q_{22} = \frac{E_{22}}{1-\upsilon_{12}\upsilon_{21}}, Q_{12} = \frac{\upsilon_{21}E_{11}}{1-\upsilon_{12}\upsilon_{21}} \tag{9}$$
$$Q_{66} = G_{12}, \quad Q_{55} = G_{13}, \quad Q_{44} = G_{23}$$

3.3 Derivation of motion equations

In this section, The Hamilton's principle is applied to produce the equations of motion. Actually, the Hamilton's principle can be defined as

$$\int_0^t (\delta U + \delta V + \delta K) dt = 0 \tag{10}$$

Where δU, δV and δK are the virtual variation of the strain energy, the virtual work done by external forces and the virtual kinetic energy.

3.3.1 Strain energy

Firstly, the variation expression of strain energy is written as

$$\delta U = \sum_{n=1}^{3} \int_{h_n}^{h_{n+1}} \int_A \sigma_{xx}\delta\varepsilon_{xx} + \sigma_{yy}\delta\varepsilon_{yy} + \sigma_{xy}\delta\gamma_{xy} + \sigma_{yz}\delta\gamma_{yz} + \sigma_{xz}\delta\gamma_{xz} \, dA dx \tag{11}$$

By substituting Eq. (7) into Eq. (11), one obtains

$$\delta U = \int_A \Big\{ N_{xx}\delta u_{0,x} - M_{xx}\delta\varphi_{x,x} + P_{xz}\delta(\varphi_x + w_{0,x}) + N_{yy}\delta v_{0,y} + M_{yy}\delta\varphi_{y,y} + P_{yz}\delta(\varphi_y + w_{0,y}) + N_{xy}(\delta u_{0,y} + \delta v_{0,x}) + M_{xy}\delta(\varphi_{x,y} + \varphi_{y,x}) \Big\} dxdy \tag{12}$$

Where the axial forces and bending moments in above equation can be defined as follows

$$(N_{xx}, N_{yy}, N_{xy}) = \sum_{n=1}^{3} \int_{h_n}^{h_{n+1}} (\sigma_{xx}, \sigma_{yy}, \sigma_{xy}) dz \tag{13a}$$

$$(M_{xx}, M_{yy}, M_{xy}) = \sum_{n=1}^{3} \int_{h_n}^{h_{n+1}} z(\sigma_{xx}, \sigma_{yy}, \sigma_{xy}) dz \tag{13b}$$

$$(P_{xz}, P_{yz}) = \sum_{n=1}^{3} \int_{h_n}^{h_{n+1}} (\sigma_{xz}, \sigma_{yz}) dz \tag{13c}$$

Now, by substituting Eq. (8) into Eq. (13), with respect to thickness direction, z- axis, one obtains the following resultant forces and moments can be achieved

$$\begin{Bmatrix} N_{xx} \\ N_{yy} \\ N_{xy} \\ M_{xx} \\ M_{yy} \\ M_{xy} \end{Bmatrix} = \begin{bmatrix} A_{11} & A_{12} & 0 & B_{11} & B_{12} & 0 \\ A_{12} & A_{22} & 0 & B_{12} & B_{22} & 0 \\ 0 & 0 & A_{66} & 0 & 0 & B_{66} \\ B_{11} & B_{12} & 0 & C_{11} & C_{12} & 0 \\ B_{12} & B_{22} & 0 & C_{12} & C_{22} & 0 \\ 0 & 0 & B_{66} & 0 & 0 & C_{66} \end{bmatrix} \begin{Bmatrix} \dfrac{\partial u_0}{\partial x} \\ \dfrac{\partial v_0}{\partial y} \\ \dfrac{\partial u_0}{\partial y} + \dfrac{\partial v_0}{\partial x} \\ \dfrac{\partial \phi_x}{\partial x} \\ \dfrac{\partial \phi_y}{\partial y} \\ \left(\dfrac{\partial \phi_x}{\partial y} + \dfrac{\partial \phi_y}{\partial x} \right) \end{Bmatrix} \tag{14a}$$

$$\begin{Bmatrix} P_{yz} \\ P_{xz} \end{Bmatrix} = \begin{bmatrix} D_{44} & 0 \\ 0 & D_{55} \end{bmatrix} \begin{Bmatrix} \phi_y + \dfrac{\partial w_0}{\partial y} \\ \phi_x + \dfrac{\partial w_0}{\partial x} \end{Bmatrix} \tag{14b}$$

Where A_{ij}, B_{ij}, C_{ij}, D_{ij}, are the plate stiffness, defined by

$$\left[A_{ij}, B_{ij}, C_{ij}\right] = \sum_{n=1}^{3} \int_{h_n}^{h_{n+1}} Q_{ij}\left[1, z, z^2\right] dz; \quad i, j = 1, 2, 6 \tag{15a}$$

$$\left[D_{ij}\right] = \sum_{n=1}^{3} \beta \int_{h_n}^{h_{n+1}} Q_{ij} dz; \quad i, j = 4, 5 \tag{15b}$$

Where β is the Timoshenko shear correction factor of the shear deformation and its exact value depending on the shape of the cross-section. Here, β for rectangular beams has been assumed to be 5/6.

3.3.2 Potential energy

Secondly, the CNTRC plates are placed on the Pasternak elastic foundation composing of the Winkler and shear layer springs. Thus, to address this problem, the virtual potential energy resulting from the bending loading q and the reaction force of foundation elastic can be written as

$$\delta V = \int_A \begin{pmatrix} -q\delta w_0 + k_w w_0 \delta w_0 \\ \\ +k_s\left(\dfrac{\partial w_0}{\partial x}\dfrac{\partial \delta w_0}{\partial x} + \dfrac{\partial w_0}{\partial y}\dfrac{\partial \delta w_0}{\partial y}\right) \end{pmatrix} dxdy \tag{16}$$

Where k_w and k_s are the corresponding spring constant factors of Winkler and shear layer respectively.

3.3.3 Virtual kinetic energy

The virtual kinetic energy of the CNTs reinforced sandwich plate with thickness h can be obtain using (Nebab *et al*. 2019)

$$\begin{aligned} \delta K &= \int_V \rho(z)\left[\dot{u}\delta\dot{u} + \dot{v}\delta\dot{v} + \dot{w}\delta\dot{w}\right] dxdydz \\ &= \int_V \left\{ I_0\left(\dot{u}_0\delta\dot{u}_0 + \dot{v}_0\delta\dot{v}_0 + \dot{w}_0\delta\dot{w}_0\right) + \right. \\ &\quad I_1\left(\dot{u}_0\delta\dot{\varphi}_x + \dot{v}_0\delta\dot{\varphi}_y + \dot{\varphi}_x\delta\dot{u}_0 + \dot{\varphi}_y\delta\dot{v}_0\right) \\ &\quad \left. + I_2\left(\dot{\varphi}_x\delta\dot{\varphi}_x + \dot{\varphi}_y\delta\dot{\varphi}_y\right)\right\} dxdy \end{aligned} \tag{17a}$$

In above equation, the mass moments of inertia can be defined as

$$\left[I_0, I_1, I_2\right] = \sum_{n=1}^{3} \int_{h_n}^{h_{n+1}} \rho(z)\left[1, z, z^2, \right] dz \tag{17b}$$

3.4 Governing equations of motion

By substituting Eqs. (12), (16) and (17) into Eq. (10), Then, integrating by parts and collecting the coefficients of δu_0, δv_0, δw_0, $\delta\varphi_x$ and $\delta\varphi_y$, leads to the following equations of motion.

$$\delta u_0 : \frac{\partial N_{xx}}{\partial x} + \frac{\partial N_{xy}}{\partial y} = I_0\ddot{u}_0 + I_1\ddot{\varphi}_x \tag{18a}$$

$$\delta v_0 : \frac{\partial N_{yy}}{\partial y} + \frac{\partial N_{xy}}{\partial x} = I_0\ddot{v}_0 + I_1\ddot{\varphi}_y \tag{18b}$$

$$\delta w_0 : \frac{\partial P_{xz}}{\partial x} + \frac{\partial P_{yz}}{\partial y} - k_w\ddot{w}_0 + k_s\left(\frac{\partial w_0^2}{\partial x^2} + \frac{\partial w_0^2}{\partial y^2}\right) + q = I_0\ddot{w}_0 \tag{18c}$$

$$\delta\varphi_x : \frac{\partial M_{xx}}{\partial x} - P_{xz} + \frac{\partial M_{xy}}{\partial y} = I_1\ddot{u}_0 + I_2\ddot{\varphi}_x \tag{18d}$$

$$\delta\varphi_y : \frac{\partial M_{yy}}{\partial y} - P_{yz} + \frac{\partial M_{xy}}{\partial x} = I_1\ddot{v}_0 + I_2\ddot{\varphi}_y \tag{18e}$$

3.5 Analytical solution

Up to now, many analytical and numerical methods are found to be utilized for the goal of solving the bending and vibration problems of simply supported CNTRC plates. In this paper, the Navier method is employed.

$$\begin{aligned} u_0(x,y,t) &= \sum_{M=1}^{\infty}\sum_{N=1}^{\infty} U_{MN}\, e^{i\omega t}\cos(\alpha x)\sin(\zeta y) \\ v_0(x,y,t) &= \sum_{M=1}^{\infty}\sum_{N=1}^{\infty} V_{MN}\, e^{i\omega t}\sin(\alpha x)\cos(\zeta y) \\ w_0(x,y,t) &= \sum_{M=1}^{\infty}\sum_{N=1}^{\infty} W_{MN}\, e^{i\omega t}\sin(\alpha x)\sin(\zeta y) \\ \varphi_x(x,y,t) &= \sum_{M=1}^{\infty}\sum_{N=1}^{\infty} \Theta x_{MN}\, e^{i\omega t}\cos(\alpha x)\sin(\zeta y) \\ \varphi_y(x,y,t) &= \sum_{M=1}^{\infty}\sum_{N=1}^{\infty} \Theta y_{MN}\, e^{i\omega t}\sin(\alpha x)\cos(\zeta y) \end{aligned} \tag{19}$$

Where $\alpha = \frac{M\pi}{a}$ and $\zeta = \frac{N\pi}{b}.i = \sqrt{-1}$

U_{MN}, and V_{MN}, W_{MN}, Θx_{MN}, Θy_{MN} are arbitrary parameters and ω is the frequency of free vibration.

The transverse load (q) is also expanded as

$$q(x,y) = \sum_{M=1}^{\infty}\sum_{N=1}^{\infty} Q_{MN}\sin(\alpha x)\sin(\zeta y) \tag{20}$$

For different types of loads acting on the CNTRC plates can be defined as

$$\text{for sinusoidal load } Q_{MN} = q_0, (M = N = 1) \tag{21}$$

$$\text{for uniform load } Q_{MN} = \frac{16q_0}{MN\pi^2}, (M = N = 1, 3, 5....) \tag{22}$$

Substituting the Eq. (19) into the Eq. (18), one obtains the closed-form solutions which are presented in the following matrix form.

$$\left(\begin{bmatrix} s_{11} & s_{12} & s_{13} & s_{14} & s_{15} \\ s_{12} & s_{22} & s_{23} & s_{24} & s_{25} \\ s_{13} & s_{23} & s_{33} & s_{34} & s_{35} \\ s_{14} & s_{24} & s_{34} & s_{44} & s_{45} \\ s_{15} & s_{25} & s_{35} & s_{45} & s_{55} \end{bmatrix} - \omega^2 \begin{bmatrix} m_{11} & m_{12} & m_{13} & m_{14} & m_{15} \\ m_{12} & m_{22} & m_{23} & m_{24} & m_{25} \\ m_{13} & m_{23} & m_{33} & m_{34} & m_{35} \\ m_{14} & m_{24} & m_{34} & m_{44} & m_{45} \\ m_{15} & m_{25} & m_{35} & m_{45} & m_{55} \end{bmatrix}\right) \begin{Bmatrix} U_{MN} \\ V_{MN} \\ W_{MN} \\ \Theta_{xMN} \\ \Theta_{yMN} \end{Bmatrix} = \begin{Bmatrix} 0 \\ 0 \\ q_{mn} \\ 0 \\ 0 \end{Bmatrix} \tag{23}$$

Table 2 Comparisons of dimensionless deflections $w^*=-(w_0/h)10^{-2}$ of square reinforced sandwich plate

a/h	V_{cnt}^*	Core UD-CNT		Core FG-CNT		face sheet UD-CNT		face sheet FG-CNT	
		Zhu *et al*. (2012)	Present	Zhu *et al*. (2012)	Present	Zhu *et al*. (2012)	Present	Zhu *et al*. (2012)	Present
10	0.11	0.3739	0.3739	0.5216	0.5228	0.3739	0.3739	0.3176	0.3177
	0.14	0.3305	0.3298	0.4512	0.4512	0.3305	0.3298	0.2842	0.2838
	0.17	0.2394	0.2394	0.3368	0.3377	0.2394	0.2394	0.2011	0.2013
20	0.11	3.6290	3.6321	6.1360	6.1587	3.6290	3.6321	2.7030	2.7041
	0.14	3.0020	2.9947	5.0530	5.0560	3.0020	2.9947	2.2580	2.2523
	0.17	2.3490	2.3514	4.0070	4.0227	2.3490	2.3514	1.7380	1.7400

Table 3 Comparisons of dimensionless frequencies ($\bar{\omega}$) of square reinforced sandwich plate under uniform loads ($V_{cnt}^* = 0.17$)

Core reinforced sandwich plate							
			a/h=5			a/h=10	
	(m,n)	(1-1)	(1-2)	(2-2)	(1-1)	(1-2)	(2-2)
Reinforcement type	Source						
UD-CNT	Present	0.4305	0.6311	0.9962	0.1678	0.2196	0.4305
	Wattanasakulpong *et al*. (2015) TSDT	0.4383	0.6372	1.0650	0.1683	0.2201	0.4383
FG-CNT	Present	0.4048	0.6100	0.9810	0.1425	0.1999	0.4048
	Wattanasakulpong *et al*. (2015) TSDT	0.3992	0.6114	0.9912	0.1409	0.1993	0.3992
Top and bottom face sheet reinforced sandwich plate							
UD-CNT	Present	0.4305	0.6311	0.9962	0.1678	0.2196	0.4305
	Wattanasakulpong *et al*. (2015) TSDT	0.4383	0.6372	1.0650	0.1683	0.2201	0.4383
FG-CNT	Present	0.4463	0.6543	1.0179	0.1824	0.2343	0.4463
	Wattanasakulpong *et al*. (2015) TSDT	0.4524	0.6552	1.0935	0.1819	0.2334	0.4524

Where

$$
\begin{aligned}
&s_{11}=-A_{11}\alpha^2+A_{66}\zeta^2,\ \ s_{12}=-\alpha\zeta(A_{12}+A_{66}),\ \ s_{13}=0,\\
&s_{14}=-B_{11}\alpha^3-B_{66}\zeta^2,\ \ s_{15}=-B_{12}\alpha\zeta-B_{66}\alpha\zeta,\ \ s_{21}=s_{12},\\
&s_{22}=-A_{66}\alpha^2-A_{22}\zeta^2,\ \ s_{23}=0,\ \ s_{24}=-B_{12}\alpha\zeta-B_{66}\alpha\zeta,\\
&s_{25}=-B_{66}\alpha^2-B_{22}\zeta^2,\ \ s_{31}=s_{13},\ \ s_{32}=s_{23},\\
&s_{33}=-D_{55}\alpha^2-D_{44}\zeta^2-k_w-k_s\left(\alpha^2+\zeta^2\right),\ \ s_{34}=-D_{55}\alpha,\\
&s_{35}=-D_{44}\zeta,\ \ s_{41}=s_{14},\ \ s_{42}=s_{24},\ \ s_{43}=s_{34},\\
&s_{44}=-C_{11}\alpha^2-C_{66}\zeta^2-D_{55},\ \ s_{45}=-\alpha\zeta(C_{12}+C_{66}),\\
&s_{51}=s_{15},\ \ s_{52}=s_{25},\ \ s_{53}=s_{35},\ \ s_{54}=s_{45},\\
&s_{55}=-D_{44}-C_{66}\alpha^2-C_{22}\zeta^2
\end{aligned}
\tag{24}
$$

And

$$
\begin{aligned}
&m_{11}=m_{22}=m_{33}=-I_0,\ \ m_{44}=m_{55}=I_2,\ \ m_{12}=m_{21}=0,\\
&m_{13}=m_{31}=0,\ \ m_{14}=m_{41}=I_1,\ \ m_{15}=m_{51}=0,\\
&m_{23}=m_{32}=0,\ \ m_{24}=m_{42}=0,\ \ m_{25}=m_{52}=I_1,\\
&m_{34}=m_{43}=0,\ \ m_{35}=m_{53}=0,\ \ m_{45}=m_{54}=0,
\end{aligned}
\tag{25}
$$

3.6 Dimensionless governing equations

It is better to clarify the dimensionless parameters used to present the results for bending and vibration analyses of CNTRC plates.

For bending problem

$$
\begin{aligned}
&\bar{w}=\frac{10^3 D_0}{q_0 a^4}w(a/2,b/2)\qquad \bar{u}=\frac{10^3 D_0}{q_0 a^4}u(0,b/2,-h/2)\\
&\bar{v}=\frac{10^3 D_0}{q_0 a^4}v(a/2,0,-h/2);\quad \bar{\sigma}_{xx}=-\frac{h^2}{q_0 a^2}\sigma_{xx}(a/2,b/2,-h/2)\\
&\bar{\sigma}_{xy}=\frac{h^2}{q_0 a^2}\sigma_{xy}(0,0,-h/2);\ \bar{\sigma}_{xz}=-\frac{h^2}{q_0 a^2}\sigma_{xz}(0,b/2,-h/2)\\
&K_w=\beta_w D_0/a^4;\quad K_s=\beta_s D_0/a^2
\end{aligned}
\tag{26}
$$

Where $D_0=\frac{E^P h^3}{12\left[1-(\nu^P)^2\right]}$

For vibration analysis

$$\bar{\omega}=\omega h\sqrt{\rho^P/E^P} \tag{27}$$

4. Results and discussions

In this section, a series of illustrations of bending and free vibrations behaviors of CNTRC sandwich plates are presented and discussed in order to explain the effect of various parameters such as geometric constants, aspect ratios, foundation parameters, carbon nanotube volume fraction, types of reinforcement, core-to-face sheet thickness ratio and types of loads acting. The effective material characteristics of CNTRC plates employed throughout this work are given as follows. PMPV (Polymer) is used as the matrix in which material properties are: ν^p=0.34, ρ^p=1150 kg/m^3 and E^P=2.1 GPa. For reinforcement material, the

Table 4 Convergence studies for deflections and stresses of square reinforced sandwich plate (h_c/h_t=2) with and without elastic foundation under uniform load ($V_{cnt}^{*} = 0.17$, a/h=10)

		Core reinforced							
		UD-CNT				FG-CNT			
	M=N	$\bar{U}$	$\bar{W}$	$\bar{\sigma}_{xx}$	$\bar{\sigma}_{xy}$	$\bar{U}$	$\bar{W}$	$\bar{\sigma}_{xx}$	$\bar{\sigma}_{xy}$
β_s=0; β_w=0	10	0.1959	1.4477	4.2894	0.1024	0.2837	1.9568	-11.8216	0.0855
	20	0.1959	1.4477	4.2897	0.1026	0.2837	1.9568	-11.8227	0.0857
	40	0.1959	1.4477	4.2898	0.1027	0.2837	1.9568	-11.8227	0.0857
	50	0.1959	1.4477	4.2898	0.1027	0.2837	1.9568	-11.8228	0.0857
β_s=50; β_w=100	10	0.0979	0.7079	2.0530	0.0553	0.1217	0.8131	-4.7355	0.0401
	20	0.0979	0.7079	2.0533	0.0555	0.1217	0.8132	-4.7364	0.0402
	40	0.0979	0.7079	2.0533	0.0556	0.1217	0.8132	-4.7365	0.0403
	50	0.0979	0.7079	2.0533	0.0556	0.1217	0.8132	-4.7366	0.0403
		Top and bottom face sheet reinforced							
β_s=0; β_w=0	10	0.0409	0.5253	0.9090	0.0373	0.0339	0.4809	1.4931	0.0423
	20	0.0409	0.5254	0.9091	0.0375	0.0339	0.4809	1.4932	0.0426
	40	0.0409	0.5254	0.9091	0.0375	0.0339	0.4809	1.4932	0.0426
	50	0.0409	0.5254	0.9091	0.0375	0.0339	0.4809	1.4932	0.0426
β_s=50; β_w=100	10	0.0297	0.3787	0.6532	0.0278	0.0252	0.3550	1.0990	0.0322
	20	0.0297	0.3788	0.6532	0.0280	0.0252	0.3550	1.0991	0.0324
	40	0.0297	0.3788	0.6532	0.0280	0.0252	0.3550	1.0991	0.0324
	50	0.0297	0.3788	0.6532	0.0280	0.0252	0.3550	1.0991	0.0324

armchair (10,10) SWCNTs is chosen with the following properties according to the study of Zhu *et al*. (2012):

$$v_{12}^{cnt} = 0.175; \rho^{cnt} = 1400kg/m^3; E_{11}^{cnt} = 5.6466TPa;$$

$$E_{22}^{cnt} = 7.0800TPa; G_{12}^{cnt} = G_{13}^{cnt} = G_{23}^{cnt} = 1.9445TPa$$

4.1 Convergence and validation studies

In this paper, the convergence and the validity of the proposed FSDT mathematical model in previous sections are established by comparing the obtained results and the existing ones in the literature which were reported by Zhu *et al*. (2012) in Table 2 for the dimensionless deflections w^*=−(w_0/h)10^{-2} and by Wattanasakulpong *et al*. (2015) for the dimensionless frequencies ($\bar{\omega}$) of square reinforced sandwich plate.

For this purposed, different values of carbon nanotube volume fraction, thickness ratio and various reinforcement of core and face sheet sandwich plate under uniform load are used. As can be seen from Table 2 and 3 the present results are in good agreement with those presented in the mentioned references. Under uniform loads with ($V_{cnt}^{*} = 0.17$) for various mode the dimensionless frequency ($\bar{\omega}$) of square reinforced sandwich plate are also presented in the Table 3. The small variation in frequency is due to the model proposed by Wattanasakulpong and Chaikittiratana (2015) which the higher-order shear deformation plate theory with an appropriate form function.

A different numbers of terms (M, N) are considered in Table 4 to give an idea of the deflections, normal stresses and shear stresses convergence results of square reinforced sandwich plate (h_c/h_t=2) under uniform load resting on Pasternak elastic foundation. The results shows that the non-dimensional deflections for Core and face sheet reinforced sandwich plate is converging well at 25th iteration, and stresses of reinforced sandwich plate have been converged at 45th and 50th iterations with and without elastic foundation.

4.2 Static deflections and stress of FG- CNT Sandwich plate

Various core and face sheet reinforcement, carbon nanotube volume fraction, uniform and sinusoidal loads are computed for square reinforced sandwich plate (h_c/h_t=2) to investigated influence of elastic foundation on the dimensionless deflections ($\bar{W}$) of plate. Maximum static deflection obtained for different parameters is given in Table 5.

It is clear that the elastic foundation on the dimensionless deflections is significant from Table 5. One can observe from this Table that a dimensionless deflection reduces in the present of elastic foundation and is less for the Pasternak foundation sort. In similar fashion, the dimensionless deflection reduces with increase in the volume fraction of carbon nanotube for all the cases. On the other hand, dimensionless deflections value with and without elastic foundation is less for FG-CNT face sheet reinforcement, high for FG-CNT core reinforcement and in between for UD-CNT core or face sheet reinforcement as clearly seen in Table 5.

Based on the results, it is clear that the FG-CNT face sheet reinforced sandwich plate has a high resistance against deflections compared to other types of reinforcement because there is a concentration of the reinforcement away from mid-plane of the sandwich plate. Based on the results, it is clear that the deflections of plates under uniform load have large compared to those of plates subjected to sinusoidal load. Additionally, these results allowed us to choose the type of reinforcement sandwich

Table 5 Effect of elastic foundation on the dimensionless deflections of square reinforced sandwich plate (h_c/h_t=2) under uniform and sinusoidal loads ($V_{cnt}^{*} = 0.17$, a/h=10)

		Core reinforced					
		Uniform load			Sinusoidal load		
β_w	β_s	Reinforcement type	$V_{cnt}^{*} = 0.11$	$V_{cnt}^{*} = 0.14$	$V_{cnt}^{*} = 0.17$	$V_{cnt}^{*} = 0.11$	$V_{cnt}^{*} = 0.14$	$V_{cnt}^{*} = 0.17$
0	0	UD-CNT	2.1638	1.9062	1.4477	1.2488	1.0932	0.8373
		FG-CNT	2.8752	2.6067	1.9568	1.6807	1.5188	1.1462
100	0	UD-CNT	1.8904	1.6896	1.3204	1.0814	0.9608	0.7593
		FG-CNT	2.4165	2.2230	1.7337	1.3991	1.2834	1.0092
100	50	UD-CNT	0.8421	0.7993	0.7079	0.4678	0.4430	0.3978
		FG-CNT	0.9338	0.9033	0.8132	0.5207	0.5037	0.4594
		Top and bottom face sheet reinforced						
0	0	UD-CNT	0.8067	0.7166	0.5254	0.4260	0.3740	0.2782
		FG-CNT	0.7417	0.6630	0.4809	0.3882	0.3435	0.2529
100	0	UD-CNT	0.7623	0.6810	0.5062	0.3996	0.3529	0.2668
		FG-CNT	0.7037	0.6323	0.4647	0.3657	0.3253	0.2433
100	50	UD-CNT	0.5058	0.4688	0.3788	0.2674	0.2460	0.2006
		FG-CNT	0.4793	0.4452	0.3551	0.2520	0.2325	0.1871

Table 6 Effect of aspect ratio (h_c/h_t) on the dimensionless deflection and stresses of square reinforced sandwich plate with and without elastic foundation under uniform load ($V_{cnt}^{*} = 0.17$, a/h=10)

		Core reinforced sandwich plate								
			UD-CNT				FG-CNT			
β_w	β_s	h_c/h_t	$\bar{U}$	$\bar{W}$	$\bar{\sigma}_{xx}$	$\bar{\sigma}_{xy}$	$\bar{U}$	$\bar{W}$	$\bar{\sigma}_{xx}$	$\bar{\sigma}_{xy}$
0	0	0.5	0.4636	2.9582	9.4161	0.2106	0.4875	3.0783	-75.9566	0.0775
		1	0.3452	2.3135	7.3480	0.1632	0.4123	2.6833	-33.3294	0.0940
		2	0.1959	1.4477	4.2898	0.1027	0.2837	1.9568	-11.8228	0.0857
100	50	0.5	0.0814	0.9359	2.8167	0.0820	0.0834	0.9474	-21.8319	0.0295
		1	0.0707	0.8556	2.7329	0.0723	0.0769	0.9061	-10.9206	0.0385
		2	0.0527	0.6746	2.2126	0.0564	0.0643	0.7946	-4.9932	0.0413
		Top and bottom face sheet reinforced sandwich plate								
0	0	0.5	0.0364	0.4839	0.8092	0.0350	0.0265	0.4204	1.1675	0.0372
		1	0.0374	0.4962	0.8317	0.0357	0.0289	0.4413	1.2707	0.0391
		2	0.0409	0.5254	0.9091	0.0375	0.0339	0.4809	1.4932	0.0426
100	50	0.5	0.0152	0.2431	0.6711	0.0229	0.0115	0.1983	1.0062	0.0238
		1	0.0156	0.2486	0.6870	0.0233	0.0124	0.2105	1.0854	0.0251
		2	0.1686	0.2649	0.7415	0.0246	0.0144	0.2350	1.2519	0.0276

plate corresponding to the applied load

The effect of aspect ratio (h_c/h_t) on the dimensionless deflection and stresses of square reinforced sandwich plate with and without elastic foundation as given in Table 6 for various reinforcement of CNTs under uniform load. It can be found that the ranges of dimensionless deflection and stresses for various Scheme or thickness of layer sandwich plate are quite different, the range is high for (h_c/h_t=2) Scheme, but the range is less for (h_c/h_t=0.5) in the case of face sheet reinforced sandwich plate and the opposite in the case of Core reinforced sandwich plate. The minimum dimensionless deflection and stresses are estimated in the case of face sheet reinforced FG-CNT and face sheet reinforced UD-CNT respectively for (h_c/h_t=0.5) in the present of elastic foundation.

In the present paper, the (Fig. 3) illustrates the dimensionless deflection ($\bar{W}$) of square reinforced sandwich plate under uniform load with fore various reinforced case with and without elastic foundation to present the effect of aspect ratio a/h. The core-to-face sheet thickness ratio is kept unchanged at (h_c/h_t=2). It can be seen from (Fig. 3(a)) and (Fig. 3(b)) that as the aspect ratio increase, the dimensionless deflection decrease then it normalize for the higher value of aspect ratio (a/h>20). For the effect of elastic foundation, the diminution of the dimensionless deflection is obvious for all case. Also, the face sheet reinforced sandwich plate has a high resistance against deflections compared to the core reinforced sandwich plate with and without elastic foundation.

It should be noted that the high resistance against deflections for the case of face sheet reinforced is attributed to a concentration of the carbon nanotube at the top and bottom layers of sandwich plate.

The effect of aspect ratio a/h and elastic foundation on the dimensionless deflection ($\bar{W}$) of square reinforced core and face sheet sandwich plate for various Scheme under uniform load is provided in the (Fig. 4). The core-to-face sheet thickness ratio is varied with the following values:

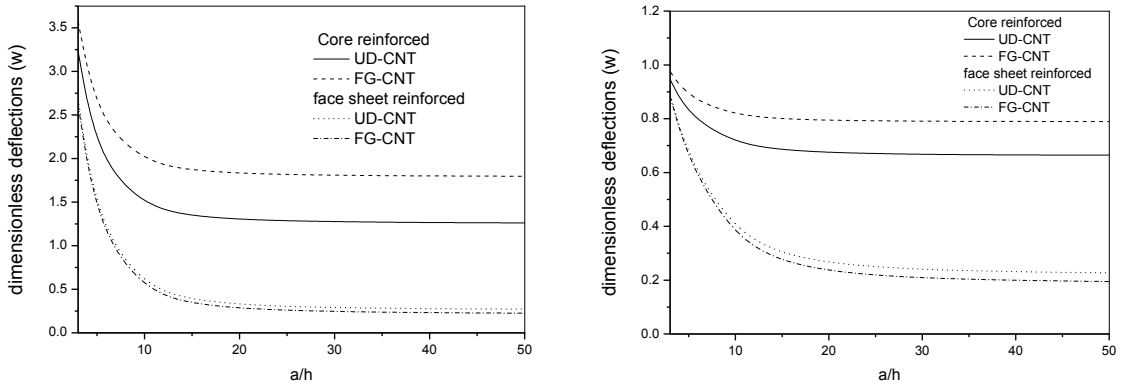

(a) β_w=0, β_s=0 (b) β_w=100, β_s=50

Fig. 3 Effect of aspect ratio a/h on the dimensionless deflection ($\bar{W}$) of square reinforced sandwich plate (h_c/h_t=2) with and without elastic foundation under uniform load ($V_{cnt}^{*} = 0.17$)

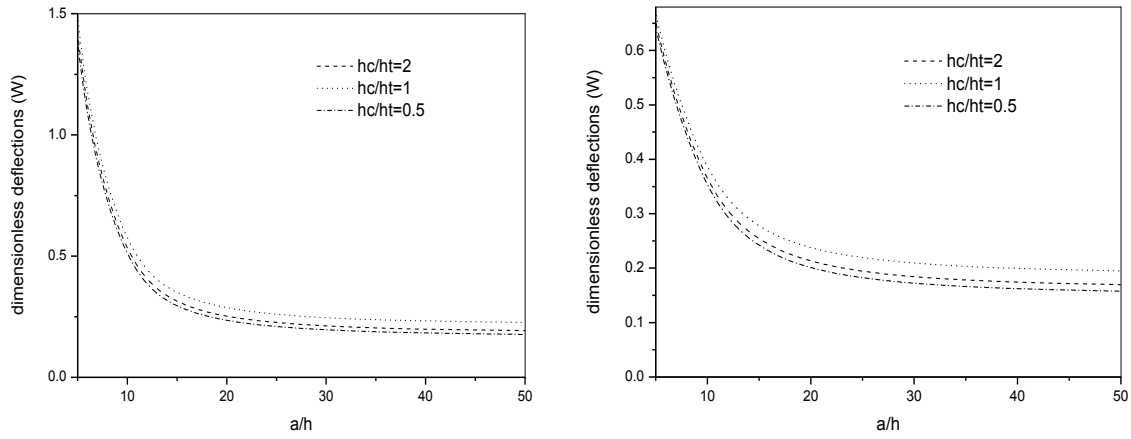

(a) β_w=0, β_s=0 (b) β_w=100, β_s=50

Fig. 4 Effect of aspect ratio *a/h* and elastic foundation on the dimensionless deflection ($\bar{W}$) of square reinforced face sheet sandwich plate for various Scheme under uniform load ($V_{cnt}^{*} = 0.17$).

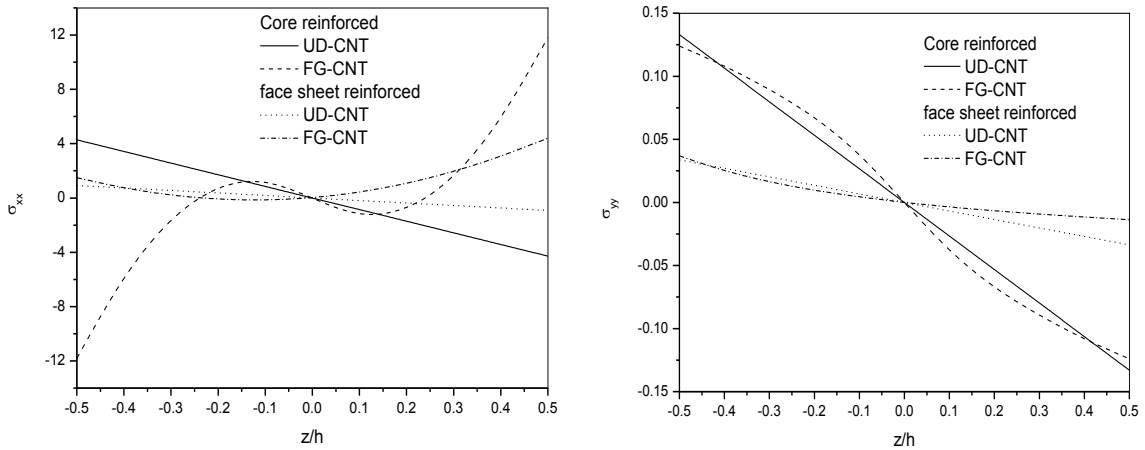

Fig. 5 Dimensionless stresses (σ_{xx} and σ_{yy}) through plate thickness of square reinforced sandwich plate ($h_c/h_t = 2$) under uniform load ($V_{cnt}^{*} = 0.17$, *a/h*=10)

(h_c/h_t=0.5, 1, 2). The values of CNTs volume fraction is considered to be equal at ($V_{cnt}^{*} = 0.17$). It is clearly seen from (Fig. 4) that the dimensionless deflection decrease once with an increase in the aspect ratio and another time with an increase in the core-to-face sheet thickness ratio for two cases with and without elastic foundation. In the other hand, it is observed that as the aspect ratio increase, the dimensionless deflection decrease rapidly (*a/h*<20) then it stabilize for the higher value. The high decrease in the dimensionless deflection is most pronounced when the plate is thick. The reason for this phenomenon is due to the fact that the shear effect is negligible for the mince plate.

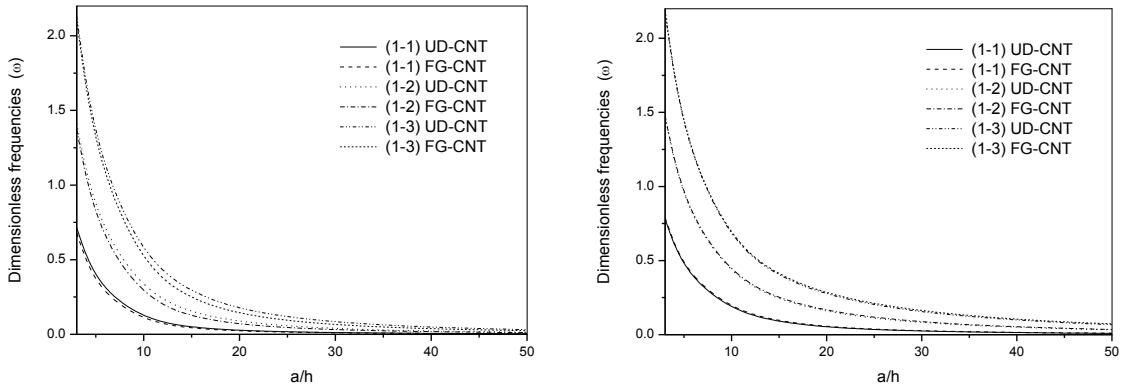

(a) reinforced core (b) reinforced face sheet

Fig. 6 Dimensionless first, second and third frequencies of square 1-2-1 sandwich plate under uniform load ($V_{cnt}^{*} = 0.17$) without elastic medium (β_w=0 , β_s=0).

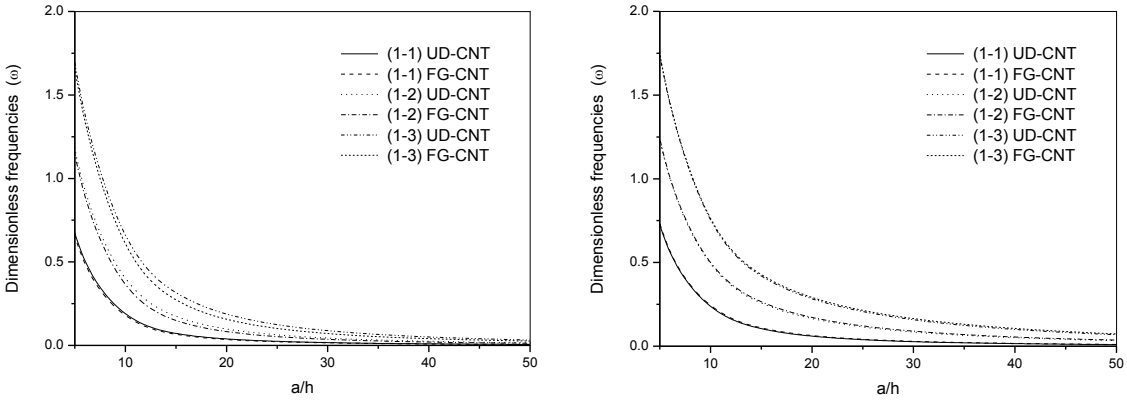

(a) reinforced core (b) reinforced face sheet

Fig. 7 Dimensionless first, second and third frequencies of square 1-2-1 sandwich plate under uniform load ($V_{cnt}^{*} = 0.17$) with elastic medium (β_w=100, β_s=50)

Influence of various reinforcement of CNTs on the axial dimensionless stresses (σ_{xx}, σ_{yy}) through plate thickness of square reinforced sandwich plate (h_c/h_t=2) under uniform load are shown in (Fig. 5) with aspect ratio (a/h=10) and nanotube volume fraction ($V_{cnt}^{*} = 0.17$). In these figures, it is observed that the dimensionless stresses vary significantly through the thickness of the plate due to the distribution function of CNTs. The sandwich reinforced plate with reinforced face sheet results in less stress and the sandwich reinforced plate with reinforced core results in high stress as clearly seen in Fig. 5. In other hand, the dimensionless stresses through plate thickness of (FG-CNT) reinforced sandwich plate are not linear and the stresses are tensile at the bottom surface and compressive at the top surface of sandwich plate.

4.3 Dimensionless frequencies of FG- CNT sandwich plate

In terms of vibration analysis, the variation of dimensionless first, second and third frequencies of square reinforced core and face sheet sandwich plate ($h_c/h_t = 2$) under uniform load with nanotube volume fraction ($V_{cnt}^{*} = 0.17$) are presented in (Fig. 6) without elastic foundation and (Fig. 7) with elastic foundation.

Their results show the dependence of dimensionless frequencies with aspect ratio, elastic foundation and various reinforcement type of sandwich plate. For every type of plates, it is expected that the frequencies the range of the dimensionless frequency increase with increasing of mode number and decrease with increasing of aspect Ratio (a/h).

More it can be seen that the difference between the dimensionless frequency of UD-CNT and FG-CNT it is very weak for all modes. In additional, the reduction in the dimensionless frequency is most pronounced in core reinforced sandwich plate. Moreover, In the presence of elastic foundation increasing the spring constant factors yields the decrease of the dimensionless frequencies of the sandwich plates.

5. Conclusions

In this research, the influence of different parameters in presence of elastic foundation on the static and dynamic behavior of carbon nanotube-reinforced composite sandwich plates was carried out using the first order shear deformation plate theory (FSDT). The structure was comprised of nanocomposite layers such as the core and face sheet reinforced. The sandwich plate was assumed to

be resting on the Pasternak elastic foundation. The rule of mixture with introducing CNT efficiency parameters has been used to estimate the effective material properties of the CNTRC. The formulations and the governing equations include the different parameters are solved and the dimensionless bending, stresses and vibration results of two types of sandwich plates resting on the Pasternak foundation which, the sandwich with face sheet reinforced and homogeneous core and the sandwich with homogeneous face sheet and reinforced core are obtained. The reliability and accuracy of the mathematical formulations model have been established through the convergence and the comparison study.

In this paper, several numerical results of bending, stresses and vibration of the sandwich plates resting on the Pasternak elastic foundation are presented and discussed in detail with different parameters such as aspect ratios, volume fraction, types of reinforcement, mode number, elastic foundation and plate thickness. The results showed the dependence of the previous parameters on the static and dynamic behavior.

Besides on the results, it is observed that:

- The dimensionless deflection reduces in the present of elastic foundation and with increase in the volume fraction of carbon nanotube for all the cases. The FG-CNT face sheet reinforced sandwich plate has a high resistance against deflections compared to other types of reinforcement because there is a concentration of the reinforcement away from mid-plane of the sandwich plate.
- The minimum dimensionless deflection and stresses are estimated in the case of face sheet reinforced FG-CNT and face sheet reinforced UD-CNT respectively for (h_c/h_t=0.5) in the present of elastic foundation.
- It should be noted that the high resistance against deflections for the case of face sheet reinforced is attributed to a concentration of the carbon nanotube at the top and bottom layers of sandwich plate.
- The high decrease in the dimensionless deflection is most pronounced when the plate is thick. The reason for this phenomenon is due to the fact that the shear effect is negligible for the mince plate.
- The range of the dimensionless frequency increase with increasing of mode number and decrease with increasing of aspect Ratio (a/h).
- The reduction in the dimensionless frequency is most pronounced in core reinforced sandwich plate and the presence of elastic foundation yields the decrease of the dimensionless frequencies of the sandwich plates.

Acknowledgments

The first Author would like to acknowledge the support provided by the Directorate General for Scientific Research and Technological Development (DGRSDT).

References

Abdulrazzaq, M.A. Kadhim, Z.D., Faleh, N.M. and Moustafa, N.M. (2020b), "A numerical method for dynamic characteristics of nonlocal porous metal-ceramic plates under periodic dynamic loads", *Struct. Monit. Mainten.*, **7**(1), 27-42. https://doi.org/10.12989/smm.2020.7.1.027

Abdulrazzaq, M.A., Fenjan, R.M., Ahmed, R.A. and Faleh, N.M. (2020a), "Thermal buckling of nonlocal clamped exponentially graded plate according to a secant function based refined theory", *Steel Compos. Struct.*, **35**(1), 147-157. https://doi.org/10.12989/scs.2020.35.1.147

Abed, Z.A.K. and Majeed, W.I. (2020), "Effect of boundary conditions on harmonic response of laminated plates", *Compos. Mater. Eng.*, **2**(2), 125-140. https://doi.org/10.12989/cme.2020.2.2.125.

Ahmed, R.A., Fenjan, R.M. and Faleh, N.M. (2019), "Analyzing post-buckling behavior of continuously graded FG nanobeams with geometrical imperfections", *Geomech. Eng.*, **17**(2), 175-180. https://doi.org/10.12989/gae.2019.17.2.175.

Ajayan, P.M., Stephen, O., Colliex, C. and Trauth, D. (1994), "Aligned carbon nanotube arrays formed by cutting a polymer resin-nanotube composite", *Sci.*, **256**, 1212-1214. https://doi.org/10.1126/science.265.5176.1212.

Al-Maliki, A.F.H., Ahmed, R.A., Moustafa, N.M. and Faleh, N.M. (2020), "Finite element based modeling and thermal dynamic analysis of functionally graded graphene reinforced beams", *Adv. Comput. Des.*, **5**(2), 177-193. https://doi.org/10.12989/acd.2020.5.2.177.

Al-Maliki, A.F.H., Ahmed, R.A., Moustafa, N.M. and Faleh, N.M. (2020), "Finite element based modeling and thermal dynamic analysis of functionally graded graphene reinforced beams", *Adv. Comput. Des.*, **5**(2), 177-193. https://doi.org/10.12989/acd.2020.5.2.177.

Al-Osta, M.A. (2019), "Shear behaviour of RC beams retrofitted using UHPFRC panels epoxied to the sides", *Comput. Concrete*, **24**(1), 37-49. https://doi.org/10.12989/cac.2019.24.1.037.

Anil, K.L., Panda, S.K., Sharma, N., Hirwani, C.K. and Topal, U. (2020), "Optimal fiber volume fraction prediction of layered composite using frequency constraints-A hybrid FEM approach", *Comput. Concrete*, **25**(4), 303-310. http://dx.doi.org/10.12989/cac.2020.25.4.303.

Arani, A.J. and Kolahchi, R. (2016), "Buckling analysis of embedded concrete columns armed with carbon nanotubes", *Comput. Concrete*, **17**(5), 567-578. http://dx.doi.org/10.12989/cac.2016.17.5.567.

Asadi, H., Souri, M. and Wang, Q. (2017), "A numerical study on flow-induced instabilities of supersonic FG-CNT reinforced composite flat panels in thermal environments", *Compos. Struct.*, **171**, 113-125. https://doi.org/10.1016/j.compstruct.2017.02.003.

Aslan, Z., Karakuzu, R. and Okutan, B. (2003), "The response of laminated composite plates under low-velocity impact loading", *Compos. Struct.*, **59**(1), 119-127. https://doi.org/10.1016/S0263-8223(02)00185-X.

Avcar, M. (2016), "Free vibration of non-homogeneous beam subjected to axial force resting on pasternak foundation", *J. Polytech.-Politeknik Dergisi.*, **19**(4), 507-512. https://doi.org/10.2339/2016.19.4.507-512.

Avcar, M. and Mohammed, W.K.M. (2018), "Free vibration of functionally graded beams resting on Winkler-Pasternak foundation", *Arab. J. Geosci.*, **11**(10), 232. https://doi.org/10.1007/s12517-018-3579-2.

Bakhshi, N. and Taheri-Behrooz, F. (2019), "Length effect on the stress concentration factor of a perforated orthotropic composite plate under in-plane loading", *Compos. Mater. Eng.*, **1**(1), 71-90. https://doi.org/10.12989/cme.2019.1.1.071.

Barati, M.R. (2019), "Vibration analysis of FG nanoplates with nanovoids on viscoelastic substrate under hygro-thermo-mechanical loading using nonlocal strain gradient theory", *Struct. Eng. Mech.*, **64**(6), 683-693.

https://doi.org/10.12989/sem.2017.64.6.683.
Barber, A.H., Cohen, S.R. and Wagner, H.D. (2003), "Measurement of carbon nanotube-polymer interfacial strength", *Appl. Phys. Lett.*, **82**, 4140-4152. https://doi.org/10.1063/1.1579568.
Barouni, A.K. and Saravanos, D.A. (2016), "A layerwise semi-analytical method for modeling guided wave propagation in laminated and sandwich composite strips with induced surface excitation", *Aerosp. Sci. Technol*., **51**, 118-141. https://doi.org/10.1016/j.ast.2016.01.023.
Behera, S. and Kumari, P. (2018), "Free vibration of Levy-type rectangular laminated plates using efficient zig-zag theory", *Adv. Comput. Des.*, **3**(3), 213-232. https://doi.org/10.12989/acd.2017.2.3.165.
Cooper, C.A., Cohen, S.R., Barber, A.H. and Wagner, H.D. (2002), "Detachment of nanotubes from a polymer matrix", *Appl. Phys. Lett*., **81**, 3873-3885. https://doi.org/10.1063/1.1521585.
Dash, S., Mehar, K., Sharma, N., Mahapatra, T.R. and Panda, S.K. (2019), "Finite element solution of stress and flexural strength of functionally graded doubly curved sandwich shell panel", *Earthq. Struct.*, **16**(1), 55-67. https://doi.org/10.12989/eas.2019.16.1.055.
Dewangan, H.C., Sharma, N., Hirwani, C.K. and Panda, S.K. (2020), "Numerical eigenfrequency and experimental verification of variable cutout (square/rectangular) borne layered glass/epoxy flat/curved panel structure", *Mech. Bas. Des. Struct. Mach*., **3**(2), 165-190. https://doi.org/10.1080/15397734.2020.1759432.
Dihaj, A., Zidour, M., Meradjah, M., Rakrak, K., Heireche, H. and Chemi, A. (2018), "Free vibration analysis of chiral double-walled carbon nanotube embedded in an elastic medium using non-local elasticity theory and Euler Bernoulli beam model", *Struct. Eng. Mech*., **65**(3), 335-342. https://doi.org/10.12989/sem.2018.65.3.335.
Duc, N.D., Cong, P.H., Tuan, N.D., Tran, P. and Van Thanh, N. (2017), "Thermal and mechanical stability of functionally graded carbon nanotubes (FG CNT)-reinforced composite truncated conical shells surrounded by the elastic foundations", *Thin Wall. Struct*., **115**, 300-310. https://doi.org/10.1016/j.tws.2017.02.016.
Eltaher, M.A. and Mohamed, S.A. (2020), "Buckling and stability analysis of sandwich beams subjected to varying axial loads", *Steel Compos. Struct*., **34**(2), 241-260. https://doi.org/10.12989/scs.2020.34.2.241.
Esawi, A.M.K. and Farag, M.M. (2007), "Carbon nanotube reinforced composites: potential and current challenges", *Mater. Des*., **28**, 2394-401. https://doi.org/10.1016/j.matdes.2006.09.022.
Gafour, Y., Hamidi, A., Benahmed, A., Zidour, M. and Bensattalah, T. (2020), "Porosity-dependent free vibration analysis of FG nanobeam using non-local shear deformation and energy principle", *Adv. Nano Res.*, **8**(1), 49-58. https://doi.org/10.12989/anr.2020.8.1.049.
Ghannadpour, S.A.M. and Mehrparvar, M. (2020), "Modeling and evaluation of rectangular hole effect on nonlinear behavior of imperfect composite plates by an effective simulation technique", *Compos. Mater. Eng*., **2**(1), 25-41. https://doi.org/10.12989/cme.2020.2.1.025.
Hadji, L., Zouatnia, N. and Bernard, F. (2019), "An analytical solution for bending and free vibration responses of functionally graded beams with porosities: Effect of the micromechanical models", *Struct. Eng. Mech.*, **69**(2), 231-241. https://doi.org/10.12989/sem.2019.69.2.231.
Hamed, M.A., Mohamed, S.A. and Eltaher, M.A. (2020), "Buckling analysis of sandwich beam rested on elastic foundation and subjected to varying axial in-plane loads", *Steel Compos. Struct*., **34**(1), 75-89. https://doi.org/10.12989/scs.2020.34.1.075.
Hamidi, A., Zidour, M., Bouakkaz, K. and Bensattalah, T. (2018), "Thermal and small-scale effects on vibration of embedded armchair single-walled carbon nanotubes", *J. Nano Res*., **51**, 24-38. https://doi.org/10.4028/www.scientific.net/JNanoR.51.24.
Hanson, G.W. (2005), "Fundamental transmitting properties of carbon nanotube antennas", *IEEE Tran. Anten. Propagat.*, **53**(11), 3426-3435. https://doi.org/10.1109/TAP.2005.858865.
Hirwani, C.K. and Panda, S.K. (2019), "Nonlinear finite element solutions of thermoelastic deflection and stress responses of internally damaged curved panel structure", *Appl. Math. Model.*, **65**, 303-317. https://doi.org/10.1016/j.apm.2018.08.014.
Hone, J., Llaguno, M.C., Nemes, N.M., Johnson, A.T., Fischer, J.E., Walters, D.A. and Smalley, R.E. (2000), "Electrical and thermal transport properties of magnetically aligned single wall carbon nanotube films", *Appl. Phys. Lett*., **77**(5), 666-668. https://doi.org/10.1063/1.127079.
Jeyaraj, P. and Rajkumar, I. (2013), "Static behavior of FG-CNT polymer nano composite plate under elevated non-uniform temperature fields", *Procedia Eng*., **64**, 825-834. https://doi.org/10.1016/j.proeng.2013.09.158.
Kar, V.R., Mahapatra, T.R. and Panda, S.K. (2015), "Nonlinear flexural analysis of laminated composite flat panel under hygro-thermo-mechanical loading", *Steel Compos. Struct.*, **19**(4), 1011-1033. http://dx.doi.org/10.12989/scs.2015.19.4.1011.
Katariya, P.V. and Panda, S.K. (2019a), "Frequency and deflection responses of shear deformable Skew sandwich curved shell panel: A finite element approach", *Arab. J. Sci. Eng.*, **44**, 1631-1648. https://doi.org/10.1007/s13369-018-3633-0.
Katariya, P.V. and Panda, S.K. (2019b), "Numerical frequency analysis of skew sandwich layered composite shell structures under thermal environment including shear deformation effects", *Struct. Eng. Mech.*, **71**(6), 657-668. http://dx.doi.org/10.12989/sem.2019.71.6.657.
Katariya, P.V., Mehar, K. and Panda, S.K. (2020), "Nonlinear dynamic responses of layered skew sandwich composite structure and experimental validation", *Int. J. Nonlin. Mech.*, 103527. https://doi.org/10.1016/j.ijnonlinmec.2020.103527.
Katariya, P.V., Panda, S.K. and Mahapatra, T.R. (2018), "Bending and vibration analysis of skew sandwich plate", *Aircraft Eng. Aerosp. Technol.*, **90**(6), 885-895. https://doi.org/10.1108/AEAT-05-2016-0087.
Katariya, P.V., Panda, S.K., Hirwani, C.K., Mehar, K. and Thakare, O. (2017), "Enhancement of thermal buckling strength of laminated sandwich composite panel structure embedded with shape memory alloy fibre", *Smart Struct. Syst.*, **20**(5), 595-605. https://doi.org/10.12989/sss.2017.20.5.595.
Keleshteri, M.M., Asadi, H. and Wang, Q. (2017), "Large amplitude vibration of FG-CNT reinforced composite annular plates with integrated piezoelectric layers on elastic foundation", *Thin Wall. Struct*., **120**, 203-214. https://doi.org/10.1016/j.tws.2017.08.035.
Kiani, Y. (2016), "Shear buckling of FG-CNT reinforced composite plates using Chebyshev-Ritz method", *Compos. Part B: Eng.*, **105**, 176-187. https://doi.org/10.1016/j.compositesb.2016.09.001.
Kiani, Y. (2017a), "Dynamics of FG-CNT reinforced composite cylindrical panel subjected to moving load", *Thin Wall. Struct.*, **111**, 48-57. https://doi.org/10.1016/j.tws.2016.11.011.
Kiani, Y. (2017b), "Free vibration of carbon nanotube reinforced composite plate on point supports using Lagrangian multipliers", *Meccanica.*, **52**(6), 1353-1367. https://doi.org/10.1007/s11012-016-0466-3.
Kiani, Y. (2017c), "Thermal buckling of temperature-dependent FG-CNT-reinforced composite skew plates", *J. Therm. Stress.*, **40**(11), 1442-1460. https://doi.org/10.1080/01495739.2017.1336742.
Kiani, Y. (2018), "Thermal post-buckling of temperature dependent sandwich plates with FG-CNTRC face sheets", *J.*

Therm. Stress., **41**(7), 866-882. https://doi.org/10.1080/01495739.2018.1425645.

Kiani, Y., Dimitri, R. and Tornabene, F. (2018), "Free vibration study of composite conical panels reinforced with FG-CNTs", *Eng. Struct.*, **172**, 472-482. https://doi.org/10.1016/j.engstruct.2018.06.006.

Kunche, M.C., Mishra, P.K., Nallala, H.B., Hirwani, C.K., Katariya, P.V., Panda, S. and Panda, S.K. (2019), "Theoretical and experimental modal responses of adhesive bonded T-joints", *Wind Struct.*, **29**(5), 361-369. http://dx.doi.org/10.12989/was.2019.29.5.361.

Lal, A., Jagtap, K.R. and Singh, B.N. (2017), "Thermo-mechanically induced finite element based nonlinear static response of elastically supported functionally graded plate with random system properties", *Adv. Comput. Des.*, **2**(3), 165-194. https://doi.org/10.12989/acd.2017.2.3.165.

Lei, Z.X., Zhang, L.W. and Liew, K.M. (2015), "Free vibration analysis of laminated FG-CNT reinforced composite rectangular plates using the kp-Ritz method", *Compos. Struct.*, **127**, 245-259. https://doi.org/10.1016/j.compstruct.2015.03.019.

Li, H., Tu, S., Liu, Y., Lu, X. and Zhu, X. (2019), "Mechanical properties of L-joint with composite sandwich structure", *Compos. Struct.*, **217**, 165-174. https://doi.org/10.1016/j.compstruct.2019.03.011.

Madani, H., Hosseini, H. and Shokravi, M. (2016), "Differential cubature method for vibration analysis of embedded FG-CNT-reinforced piezoelectric cylindrical shells subjected to uniform and non-uniform temperature distributions", *Steel Compos. Struct.*, **22**(4), 889-913. https://doi.org/10.12989/scs.2016.22.4.889.

Mahapatra, T.R., Mehar, K., Panda, S.K., Dewangan, S. and Dash, S. (2017), "Flexural strength of functionally graded nanotube reinforced sandwich spherical panel", *IOP Conf. Ser.: Mater. Sci. Eng.*, **178**(1), 012031. https://doi.org/10.1088/1757-899X/178/1/012031.

Mehar, K. and Panda, S.K. (2017a), "Thermoelastic analysis of FG-CNT reinforced shear deformable composite plate under various loading", *Int. J. Comput. Meth.*, **14**(2), 1750019. https://doi.org/10.1142/S0219876217500190.

Mehar, K. and Panda, S.K. (2017b), "Nonlinear static behavior of FG-CNT reinforced composite flat panel under thermomechanical load", *J. Aerosp. Eng.*, **30**(3), 04016100. https://doi.org/10.1061/(ASCE)AS.1943-5525.0000706.

Mehar, K. and Panda, S.K. (2018a), "Thermoelastic flexural analysis of FG-CNT doubly curved shell panel", *Aircraft Eng. Aerosp. Technol.*, **90**(1), 11-23. https://doi.org/10.1108/AEAT-11-2015-0237.

Mehar, K. and Panda, S.K. (2018b), "Elastic bending and stress analysis of carbon nanotube-reinforced composite plate: Experimental, numerical, and simulation", *Adv. Polym. Technol.*, **37**(6), 1643-1657. https://doi.org/10.1002/adv.21821.

Mehar, K. and Panda, S.K. (2020), "Nonlinear deformation and stress responses of a graded carbon nanotube sandwich plate structure under thermoelastic loading", *Acta Mech.*, **231**, 1105-1123. https://doi.org/10.1007/s00707-019-02579-5.

Mehar, K., Mishra, P.K. and Panda, S.K. (2020a), "Numerical investigation of thermal frequency responses of graded hybrid smart nanocomposite (CNT-SMA-Epoxy) structure", *Mech. Adv. Mater. Struct.*, 1-13. https://doi.org/10.1080/15376494.2020.1725193.

Mehar, K., Panda, S.K. and Mahapatra, T.R. (2017), "Theoretical and experimental investigation of vibration characteristic of carbon nanotube reinforced polymer composite structure", *Int. J. Mech. Sci.*, **133**, 319-329. https://doi.org/10.1016/j.ijmecsci.2017.08.057.

Mehar, K., Panda, S.K. and Patle, B.K. (2018), "Stress, deflection, and frequency analysis of CNT reinforced graded sandwich plate under uniform and linear thermal environment: A finite element approach", *Polym. Compos.*, **39**(10), 3792-3809. https://doi.org/10.1002/pc.24409.

Mehar, K., Panda, S.K. and Sharma, N. (2020b), "Numerical investigation and experimental verification of thermal frequency of carbon nanotube-reinforced sandwich structure", *Eng. Struct.*, **211**, 110444. https://doi.org/10.1016/j.engstruct.2020.110444.

Merzoug, M., Bourada, M., Sekkal, M., Abir, A.C., Chahrazed, B., Benyoucef, S. and Benachour, A. (2020), "2D and quasi 3D computational models for thermoelastic bending of FG beams on variable elastic foundation: Effect of the micromechanical models", *Geomech. Eng.*, **22**(4), 361-374. http://dx.doi.org/10.12989/gae.2020.22.4.361.

Mirjavadi, S.S., Forsat, M., Barati, M.R., Abdella, G.M., Mohasel Afshari, B., Hamouda, A.M.S. and Rabby, S. (2019). "Dynamic response of metal foam FG porous cylindrical micro-shells due to moving loads with strain gradient size-dependency", *Eur. Phys. J. Plus*, **134**(5), 1-11. https://doi.org/10.1140/epjp/i2019-12540-3.

Mirzaei, M. and Kiani, Y. (2016), "Thermal buckling of temperature dependent FG-CNT reinforced composite plates", *Meccanica*. **51**(9), 2185-2201. https://doi.org/10.1007/s11012-015-0348-0.

Mohammadzadeh-Keleshteri, M., Asadi, H. and Aghdam, M.M. (2017), "Geometrical nonlinear free vibration responses of FG-CNT reinforced composite annular sector plates integrated with piezoelectric layers", *Compos. Struct.*, **171**, 100-112. https://doi.org/10.1016/j.compstruct.2017.01.048.

Monge, J.C., Mantari, J.L., Yarasca, J. and Arciniega, R.A. (2019), "On bending response of doubly curved laminated composite shells using hybrid refined models", *J. Appl. Comput. Mech.*, **5**(5), 875-899. https://doi.org/10.22055/jacm.2019.27297.1397.

Narwariya, M., Choudhury, A. and Sharma, A.K. (2018), "Harmonic analysis of moderately thick symmetric cross-ply laminated composite plate using FEM", *Adv. Comput. Des.*, **3**(2), 113-132. https://doi.org/10.12989/acd.2018.3.2.113.

Nebab, M., Ait Atmane, H., Bennai, R. and Tahar, B. (2019), "Effect of nonlinear elastic foundations on dynamic behavior of FG plates using four-unknown plate theory", *Earthq. Struct.*, **17**(5), 447-462. https://doi.org/10.12989/eas.2019.17.5.447.

Nejadi, M.M. and Mohammadimehr, M. (2020), "Analysis of a functionally graded nanocomposite sandwich beam considering porosity distribution on variable elastic foundation using DQM: Buckling and vibration behaviors", *Comput. Concrete*, **25**(3), 215-224. https://doi.org/10.12989/cac.2020.25.3.215.

Odegard, G.M., Gates, T.S., Wise, K.E., Park, C. and Siochi, E.J. (2003), "Constitutive modelling of nanotube-reinforced polymer composites", *Compos. Sci. Technol.*, **63**, 1671-1687. https://doi.org/10.1016/S0266-3538(03)00063-0.

Othman, M. and Fekry, M. (2018), "Effect of rotation and gravity on generalized thermo-viscoelastic medium with voids", *Multidisc. Model. Mater. Struct.*, **14**(2), 322-338. https://doi.org/10.1108/MMMS-08-2017-0082.

Panda, S.K. and Katariya, P.V. (2015), "Stability and Free Vibration Behaviour of Laminated Composite Panels Under Thermo-mechanical Loading", *Int. J. Appl. Comput. Math.*, **1**, 475-490. https://doi.org/10.1007/s40819-015-0035-9.

Panda, S.K. and Singh, B.N. (2010), "Thermal post-buckling analysis of a laminated composite spherical shell panel embedded with shape memory alloy fibres using non-linear finite element method", *Proc. Inst. Mech. Eng., Part C: J. Mech. Eng. Sci.*, **224**(4), 757-769. https://doi.org/10.1243/09544062JMES1809.

Pandey, H.K., Agrawal, H., Panda, S.K., Hirwani, C.K., Katariya, P.V. and Dewangan, H.C. (2020), "Experimental and numerical bending deflection of cenosphere filled hybrid (Glass/Cenosphere/Epoxy) composite", *Struct. Eng. Mech.*, **73**(6), 715-724. http://dx.doi.org/10.12989/sem.2020.73.6.715.

Pandey, H.K., Hirwani, C.K., Sharma, N., Katariya, P.V. and Panda, S.K. (2019), "Effect of nano glass cenosphere filler on hybrid composite eigenfrequency responses-An FEM approach and experimental verification", *Adv. Nano Res.*, **7**(6), 419-429. http://dx.doi.org/10.12989/anr.2019.7.6.419.

Panjehpour, M., Loh, E.W.K. and Deepak, T.J. (2018), "Structural insulated panels: State-of-the-art", *Trend. Civil Eng. Arch.*, **3**(1) 336-340. https://doi.org/10.32474/TCEIA.2018.03.000151.

Patnaik, S.S., Swain, A. and Roy, T. (2020), "Creep compliance and micromechanics of multi-walled carbon nanotubes based hybrid composites", *Compos. Mater. Eng.*, **2**(2), 141-152. https://doi.org/10.12989/cme.2020.2.2.141.

Rachedi, M.A., Benyoucef, S., Bouhadra, A., Bachir Bouiadjra, R., Sekkal, M. and Benachour, A. (2020), "Impact of the homogenization models on the thermoelastic response of FG plates on variable elastic foundation", *Geomech. Eng.*, **22**(1), 65-80. http://dx.doi.org/10.12989/gae.2020.22.1.065.

Rahmani, M., Mohammadi, Y., Kakavand, F. and Raeisifard, H. (2020), "Vibration analysis of different types of porous FG conical sandwich shells in various thermal surroundings", *J. Appl. Comput. Mech.*, **6**(3), 416-432. https://doi.org/10.22055/jacm.2019.29442.1598.

Ranjbartoreh, A.R., Ghorbanpour, A. and Soltani, B. (2007), "Double-walled carbon nanotube with surrounding elastic medium under axial pressure", *Physica E: Lowdimens. Syst. Nanostruct.*, **39**(2), 230-239. https://doi.org/10.1016/j.physe.2007.04.010.

Reddy, J.N. (2004), *Mechanics of Laminated Composite Plates and Shells: Theory and Analysis*, 2nd Edition, CRC Press, Taylor & Francis eBooks.

Rezaiee-Pajand, M., Masoodi, A.R. and Mokhtari, M. (2018), "Static analysis of functionally graded non-prismatic sandwich beams", *Adv. Comput. Des.*, **3**(2), 165-190. https://doi.org/10.12989/acd.2018.3.2.165.

Safa, A., Hadji, L., Bourada, M. and Zouatnia, N. (2019), "Thermal vibration analysis of FGM beams using an efficient shear deformation beam theory", *Earthq. Struct.*, **17**(3), 329-336. https://doi.org/10.12989/eas.2019.17.3.329.

Sahmani, S. and Fattahi, A.M. (2017), "Nonlocal size dependency in nonlinear instability of axially loaded exponential shear deformable FG-CNT reinforced nanoshells under heat conduction", *Eur. Phys. J. Plus*, **132**(5), 231. https://doi.org/10.1140/epjp/i2017-11497-5.

Sahoo, S.S., Panda, S.K. and Singh, V.K. (2017), "Experimental and numerical investigation of static and free vibration responses of woven glass/epoxy laminated composite plate", *Proc. Inst. Mech. Eng., Part L: J. Mater. Des.*, **231**(5), 463-478. https://doi.org/10.1177/1464420715600191.

Sahoo, S.S., Singh, V.K. and Panda, S.K. (2016), "Nonlinear flexural analysis of shallow carbon/epoxy laminated composite curved panels: experimental and numerical investigation", *J. Eng. Mech.*, **142**(4), 04016008. https://doi.org/10.1061/(ASCE)EM.1943-7889.0001040.

Sahouane, A., Hadji, L. and Bourada, M. (2019), "Numerical analysis for free vibration of functionally graded beams using an original HSDBT", *Earthq. Struct.*, **17**(1), 31-37. https://doi.org/10.12989/eas.2019.17.1.031.

Sahu, P., Sharma, N. and Panda, S.K. (2020), "Numerical prediction and experimental validation of free vibration responses of hybrid composite (Glass/Carbon/Kevlar) curved panel structure", *Compos. Struct.*, **241**, 112073. https://doi.org/10.1016/j.compstruct.2020.112073.

Sayyad, A. and Ghumare, S. (2019), "A new Quasi-3D model for functionally graded plates", *J. Appl. Comput. Mech.*, **5**(2), 367-380. https://doi.org/10.22055/jacm.2018.26739.1353.

Selmi, A. (2019), "Effectiveness of SWNT in reducing the crack effect on the dynamic behavior of aluminium alloy", *Adv. Nano Res.*, **7**(5), 365-377. https://doi.org/10.12989/anr.2019.7.5.365.

Shen, H.S. (2009), "Nonlinear bending of functionally graded carbon nanotube reinforced composite plates in thermal environments", *Compos Struct.*, **91**, 9-19. https://doi.org/10.1016/j.compstruct.2009.04.026.

Shokravi, M. (2017), "Buckling of sandwich plates with FG CNT-reinforced layers resting on orthotropic elastic medium using Reddy plate theory", *Steel Compos. Struct.*, **23**(6), 623-631. https://doi.org/10.12989/scs.2017.23.6.623.

Shokrieh, M.M. and Kondori, M.S. (2020), "Effects of adding graphene nanoparticles in decreasing of residual stresses of carbon/epoxy laminated composites", *Compos. Mater. Eng.*, **2**(1), 53-64. https://doi.org/10.12989/cme.2020.2.1.053.

Verma, K.L. (2013), "Wave propagation in laminated composite plates", *Int. J. Adv. Struct. Eng.*, **5**(1), 10. https://doi.org/10.1186/2008-6695-5-10.

Vodenitcharova, T. and Zhang, L.C. (2006), "Bending and local buckling of a nanocomposite beam reinforced by a single-walled carbon nanotube", *Int. J. Solid. Struct.*, **43**, 3006-3024. https://doi.org/10.1016/j.ijsolstr.2005.05.014.

Wattanasakulpong, N. and Chaikittiratana, A. (2015), "Exact solutions for static and dynamic analyses of carbon nanotube-reinforced composite plates with Pasternak elastic foundation", *Appl. Math. Model.*, **39**(18), 5459-5472. https://doi.org/10.1016/j.apm.2014.12.058.

Xie, S., Li, W., Pan, Z., Chang, B. and Sun, L. (2000), "Mechanical and physical properties on carbon nanotube", *J. Phys. Chem. Solid.*, **61**(7), 1153-1158. https://doi.org/10.1016/S0022-3697(99)00376-5.

Zhang, L.W., Lei, Z.X. and Liew, K.M. (2015), "Buckling analysis of FG-CNT reinforced composite thick skew plates using an element-free approach", *Compos. Part B: Eng.*, **75**, 36-46. https://doi.org/10.1016/j.compositesb.2015.01.033.

Zhu, P., Lei, Z.X. and Liew, K.M. (2012), "Static and free vibration analyses of carbon nanotube reinforced composite plates using finite element method with first order shear deformation plate theory", *Compos. Struct.*, **94**, 1450-1460. https://doi.org/10.1016/j.compstruct.2011.11.010.

CC